Proceedings of the ASME 2019 International Design Engineering Technical Conferences and Computers and Information in Engineering Conferences
IDETC2019
August 18-21, 2019, Anaheim, California, USA

IDETC2019-98118

DESIGN OF AN UNDERACTUATED LEGGED ROBOT WITH PRISMATIC LEGS FOR PASSIVE ADAPTABILITY TO TERRAIN

Seonghoon Noh
Yale University
Department of Mechanical Engineering
New Haven, Connecticut, USA
seonghoon.noh@yale.edu

Aaron Dollar
Yale University
Department of Mechanical Engineering
New Haven, Connecticut, USA
aaron.dollar@yale.edu

ABSTRACT

Legged robots have the advantage of being able to maneuver rough, unstructured terrains unlike their wheeled counterparts. However, many legged robots require multiple sensors and online computations to specify the gait, trajectory or contact forces in real-time for a given terrain, and these methods can break down when sensory information is unreliable or not available. Over the years, underactuated mechanisms have demonstrated great success in object grasping and manipulation tasks due to their ability to passively adapt to the geometry of the objects without sensors. In this paper, we present an application of underactuation in the design of a legged robot with prismatic legs that maneuvers unstructured terrains under open-loop control using only four actuators – one for stance for each half of the robot, one for forward translation, and one for steering. Through experimental results, we show that prismatic legs can support a statically stable stance and can facilitate locomotion over unstructured terrain while maintaining its body posture.

INTRODUCTION

Legged robots have greatly improved over the years in their ability to quickly, stably and efficiently maneuver different terrains. Because a predefined trajectory cannot be applied for an arbitrary terrain, many legged robots incorporate a control framework that performs online trajectory planning using sensor information about the environment. As such, they are equipped with one or more sensing modalities and a redundant number of actuators to follow the computed trajectory. One example is the MIT Cheetah 3 that uses a policy-regularized model predictive control to maneuver unstructured terrains [1]. While such methods enable impressive dynamic maneuvers, they become ineffective when the sensor information is unreliable or unavailable. The high number of actuators necessary for these robots also increases the weight and power consumption.

Conversely, underactuated mechanisms have been used in simple open-loop control to complete certain tasks such as object grasping and manipulation by leveraging the natural dynamics of the mechanism. The general lack of sensors makes these systems mechanically robust since they are not dependent on sensors for operation. Furthermore, underactuation makes a mechanism passively adaptive because some internal degrees of freedom are affected both by the actuator and the environment through physical contact. In the context of legged robots, passive adaptability through underactuation may provide a solution for maneuvering unstructured terrain using a fewer number of actuators.

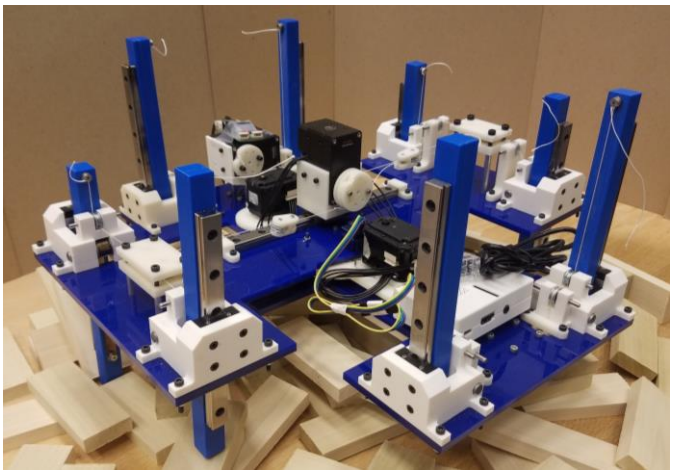

Figure 1. The underactuated legged robot standing on an unstructured obstacle course.

Early legged robots that utilized passive adaptability include RHex [2], a low-profile, six-legged robot with compliant, arched legs that rotate out of phase to travel over rough terrain, and Sprawlita [3], a biomimetic, underactuated robot composed of two tripods, each driven by a pneumatic actuator. More recent underactuated legged robots include MARLO [4], an underactuated bipedal robot that uses feedback control, and LoadRoACH [5], a 55 g hexapod crawling robot. However, the

task of maintaining the body's posture over an uneven terrain has not been considered by these underactuated legged robots, for which it is especially challenging since even a robot with fully actuated legs is underactuated in the 6-DoF space.

In this paper, we present the design of an underactuated legged robot with eight prismatic legs that can maneuver unstructured terrains under open-loop control through a quasi-static locomotion. We first discuss the leg kinematics and underactuation of the legs. We then present the novel leg design motivated by the energy model of the robot and discuss an appropriate locomotion strategy guided by the energy stability margin. The mechanical design of the robot and its core components are described. We demonstrate through experimental results that the robot can maintain its body posture over uneven terrains. Lastly, we note the limitations of the current design and possible future works.

LEG KINEMATICS

Kinematic synthesis for an underactuated legged robot must produce a leg design that can guarantee stability throughout locomotion although some degrees of freedom in the legs cannot be directly controlled. Though there exist many stability measures which will be discussed later in this paper, let us for now consider two instances of instability: slipping and toppling.

In their previous work [6], Kanner and Dollar determined the optimal kinematic parameters for an underactuated RR (revolute-revolute) leg of a cable-driven robot with a statically stable gait. They evaluated the vertical range of the leg and the ground reaction forces as the performance metrics of the optimization. They concluded that an RR leg that predominantly behaves as a single prismatic link maximizes the vertical reach and minimizes the horizontal component of the ground reaction force. Kanner et al. subsequently designed a quadruped robot with underactuated URS (universal-revolute joints with spherical ground contact) legs with an elastic four-bar linkage using parallel extension springs to maintain a vertical orientation of the distal link of the leg [7]. The quadruped robot maintained a statically stable stance with three legs while moving the fourth leg forward to achieve locomotion. Kanner et al. demonstrated in [7] that an underactuated legged robot using a statically stable stance has limited gait choices and locomotion speed due to the robot's center of mass escaping the support polygon easily.

The loss of stability in the aforementioned quadruped [7] can be attributed to two underlying limitations. First, the URS legs on the robot were optimized for a statically stable stance by remaining vertical. Therefore, placing a leg forward during locomotion would cause the other legs to rotate and to become more likely to slip or fall on the terrain. Second, underactuation reduces the control authority in the URS legs in which stance and locomotion are coupled. One solution may be to instead opt for purely prismatic legs and to decouple stance and locomotion by introducing a standalone locomotion mechanism. In this work, we expand upon the implications of the optimization results and the URS legs by designing an underactuated legged robot with prismatic legs for maneuvering unstructured terrains.

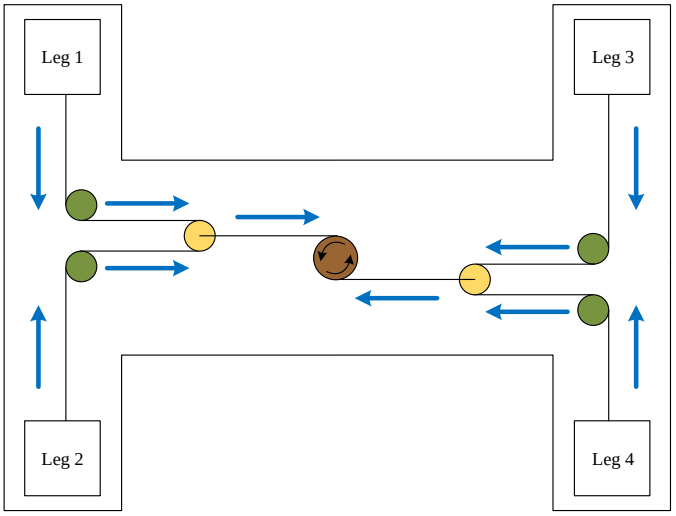

Figure 2. A schematic of the actuation cable routing for the pulley differential mechanism on the upper platform. Fixed pulleys (green) redirect the cables to the floating pulley blocks (yellow) actuated by the motor (brown).

The robot presented here has a total of eight prismatic legs, four on each of the two platforms. Because the vertically-oriented prismatic legs cannot produce any forward motion, locomotion is achieved by joining two quadruped platforms one on top of another and translating one platform in swing phase while keeping the other in stance phase. While a stable stance only requires a minimum of three legs, resulting in a total of six legs, underactuation in this robot is realized through pairwise pulley differentials as shown in Figure 2. Therefore, having four legs on each platform greatly simplifies the cable routing as opposed to having three legs.

Figure 2 shows that opposing legs on a single platform are adaptively coupled via a pulley differential. The two resulting pulley differentials are adaptively coupled once again to be actuated together by a single motor. By actuating all four legs of a stance platform with one motor, they can passively adapt to the terrain while subject to the following kinematic constraint

$$2r_m\Delta\theta_m = q_1 + q_2 + q_3 + q_4 \tag{1}$$

where the left-hand side of the equation represents the total actuated length of the two cables directly connected to the motor and the right-hand side represents the sum of the linear displacements of the four prismatic legs.

Adaptive coupling through the pulley differentials is defined by the front and rear cable length constraints below.

$$\ell_f = q_1 + q_2 \tag{2}$$
$$\ell_r = q_3 + q_4 \tag{3}$$

Since the four legs in swing phase do not interact with the terrain, Equations 1 to 3 are only of interest for the stance legs. Although these kinematic constraints allow passive adaptability

to the terrain, they do not indicate whether stability will be guaranteed on an arbitrary terrain. For this, we now consider the energy model of the robot, followed by a description of the full leg mechanism as a consequence of the energy model.

ENERGY MODEL OF THE ROBOT

Over the years, the principle of minimum energy has been applied to underactuated mechanisms to model their behavior since they are underconstrained systems that move towards the minimum energy state at any given instance while subject to kinematic constraints and friction. In this work, we apply this principle to synthesize the underactuated leg mechanism.

Consider a stance platform that uses a linear spring for each leg to keep the cable taut and to provide the restoring force for returning the legs during swing phase. By assuming a quasi-static motion and negligibility of friction, we can represent the total energy of the robot as follows:

$$E = mgh_{CoM} + \sum_{i=1}^{4} \frac{1}{2} k {q_i}^2 \tag{4}$$

where m is the total mass of the robot, h_{CoM} is the height of the center of mass, k is the stiffness of the spring, and q_i is the linear displacement of the i^{th} prismatic leg in stance phase.

We note from Equation 4 that the robot will assume a configuration that minimizes the sum of elastic potential energies in the springs. However, the energy model does not give a clear indication of the robot's steady-state body orientation on an arbitrary terrain. Furthermore, one may understand that it is not possible to meaningfully manipulate the variables such as the height of the center of mass or the individual leg displacements to design a minimum energy state that can maintain the posture of the robot in open-loop control. Common leveling or balancing methods such as moving a counterweight on the robot or coordinating the actuation of the legs become impossible. Therefore, the design of the leg mechanism must be changed accordingly to reshape the energy function. This naturally leads to the only remaining quantity we may prescribe in Equation 4, which is the elastic behavior of the spring.

To better understand the implications of the choice of a linear extension spring, consider the robot described by Equation 4 encountering an incline while walking on an even terrain. The minimum energy state described by Equation 4 indicates that the robot will transition from a horizontally level orientation to an orientation close to the slope of the incline as the stance and swing legs switch to minimize the sum of the elastic potential energies. There exist other examples of more complicated terrains, but this example illustrates that the minimum energy state described by Equation 4 is not one that minimizes the change in the robot body's orientation but one that minimizes the difference in the linear displacement of the legs. Therefore, a robot whose total energy is described by Equation 4 cannot always maintain its body posture while passively adapting to an arbitrary terrain.

While the cable-driven actuation mechanism requires the springs' antagonistic force to keep the tension in the cables, its restoring force that increases linearly with the leg's displacement poses a challenge in passively adapting to a terrain that may have great height variations between each foothold. We therefore mitigate this behavior by instead using a constant force spring. As the name suggests, constant force springs are characterized by a nearly constant restoring force after some initial extension regardless of any additional extension. Consequently, Equation 4 can now be rewritten as follows:

$$E = mgh_{CoM} + \sum_{i=1}^{4} H(q_i - x_0) k q_i \tag{5}$$

where H is the unit step function for x_0, the point of extension past which the spring assumes a nearly constant force and k is the constant force exerted by the spring.

Equation 5 shows that the elastic potential energy of the constant force springs has a linear dependence on the extension of the prismatic legs as opposed to a quadratic dependence as in Equation 4 with linear extension springs. Moreover, we observe that the new energy function in Equation 5 allows the total actuated cable length to be arbitrarily distributed among the legs without increasing in energy as long as the motion satisfies the kinematic constraints and keeps the center of mass height constant. With this condition provided by the new energy function in Equation 5, we now discuss our proposed actuation scheme for minimizing the body posture change through passive terrain adaptability.

PASSIVE TERRAIN ADAPTABILITY

Analyzing the energy model of the underactuated legged robot in the previous section resulted in a leg design capable of a greater range of reconfigurations for a given energy level through the pulley differential mechanism. We now consider the ground contact constraints, which were not explicitly given by the energy model, and their effect on passive terrain adaptability.

Consider the robot over an uneven terrain in static equilibrium with one platform in stance phase and another in swing phase. After the swing phase platform translates a certain distance, the two platforms must switch their phase to complete the gait cycle. During switching, the sum of forces and the sum of moments about the robot's center of mass are as follows:

$$\Sigma \boldsymbol{F} = \sum_{i=1}^{4} \boldsymbol{f}_i + \sum_{j=1}^{4} \boldsymbol{f}_j - mg \tag{6}$$

$$\Sigma \boldsymbol{\tau} = \sum_{i=1}^{4} (\boldsymbol{p}_i - \boldsymbol{c}) \times \boldsymbol{f}_i + \sum_{j=1}^{4} (\boldsymbol{p}_j - \boldsymbol{c}) \times \boldsymbol{f}_j \tag{7}$$

where $\boldsymbol{f}_i$ and $\boldsymbol{f}_j$ are the contact forces on the i^{th} stance leg and the j^{th} swing leg respectively, $\boldsymbol{p}_i$ and $\boldsymbol{p}_j$ are the coordinates of

the i^{th} stance foot and the j^{th} swing foot respectively, and $\boldsymbol{c}$ is the coordinate of the center of mass.

Since the robot is initially in static equilibrium by assumption, the value of the contact forces on the swing legs will determine whether the robot will remain in static equilibrium during switching. Now, let us consider the sum of forces on a single leg, which includes the actuation cable tension, contact force and the spring force with the contact force being zero for a leg not on the ground.

$$\Sigma \boldsymbol{F}_{leg} = \boldsymbol{F}_c - \boldsymbol{f} - \boldsymbol{F}_s \tag{8}$$

From Equations 6 to 8, one can observe that the sum of moments can become nonzero for several reasons during the switching process. Despite the net force on the swing legs before contact being equal in theory, friction in the system and variations in the terrain elevation will result in asynchronous ground contact. Therefore, a robot initially in static equilibrium can experience a resultant moment as contact forces on the swing legs become nonzero.

We therefore propose an actuation scheme in which the swing legs are initially actuated in position control with a torque limit. The commanded position during this time lies between the swing leg position and the stance leg position. The value of the torque limit is experimentally determined and is enough to overcome the internal friction and the constant spring force but not enough to overcome the portion of the robot weight to be support at the leg. Through this actuation scheme, we can ensure that further actuation will result in the legs passively adapting to the terrain while inducing minimal moment on the robot body.

While this intermediate actuation phase cannot guarantee that all swing legs will contact the ground on an arbitrary terrain, it is necessary to minimize the net moment on the robot during switching. After this intermediate phase, the swing legs are actuated to full extension without the torque limit. With this actuation scheme for the swing legs, we now synthesize the complete alternating stance gait for the underactuated legged robot.

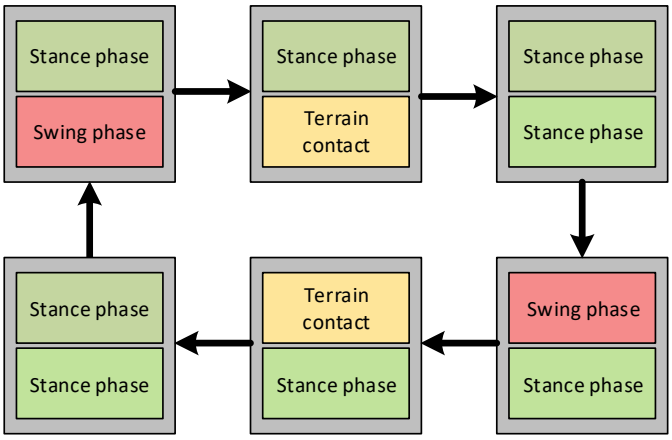

Figure 3. A diagram showing the alternating stance gait with the intermediate actuation phase. The upper and lower boxes represent the phase of the upper and lower quadruped platforms respectively. The arrows represent the relative translation between the two platforms.

GAIT SYNTHESIS

Underactuation of the legs justifies the separation of the stance and locomotion mechanisms as explained previously, but the choice of prismatic legs as presented in this work now requires the separation because the legs can only move perpendicularly to the direction of locomotion. Whereas the actuation of the prismatic legs affects the z-coordinate of the robot body's centroid and the roll and pitch angles through reconfiguration and adaptation to the terrain, the decoupled locomotion mechanism only affects the x-coordinate, y-coordinate, and the yaw angle of the swing phase platform with respect to the stance phase platform through relative translation and rotation. This is known as an alternating stance gait, in which the stance legs maintain static equilibrium while the swing legs move forward to become the new stance legs. To this alternating stance gait, we now add the intermediate phase during which the actuation scheme for the swing legs is executed as described in the previous section. Therefore, a complete gait cycle for the underactuated legged robot can be represented by the state transition diagram in Figure 3.

ENERGY STABILITY MARGIN IN UNDERACTUATED LEGGED ROBOTS

The stability of a legged robot may be one of the most important performance metrics as it ensures the continuation of successful locomotion over a terrain. For any given legged robot, its center of gravity may be projected onto a horizontal plane and a convex polygon consisted of the points of ground contact known as the support pattern or support polygon may be created. MgGhee and Frank formally defined the stability margin associated with a line segment of the support polygon of a legged robot as the distance between the projected center of gravity and the line segment [8]. The stability of the robot could then be assessed by the line segment with the lowest stability margin. However, Messuri and Klein noted that the stability margin fails to account for an uneven terrain and subsequently proposed the energy stability margin for the line segments of a support boundary [9].

A support boundary differs from the support polygon in that it does not lie in a horizontal plane but is a convex hull formed by the lines connecting the footholds on an uneven terrain in 3D space, thus better representing stability on an uneven terrain. The energy stability margin for a line segment of a support boundary is then defined as the energy required to rotate the center of gravity over the line segment, i.e. the difference between the potential energy at the instant of toppling and the potential energy at the initial state. Hirose et al. further noted that the weight of a robot does not affect its tendency to tumble and proposed an energy stability margin normalized by the weight [10].

We briefly present the derivation of the normalized stability margin and discuss its effect on the gait parameters. For every line segment of the support boundary in the Euclidean space

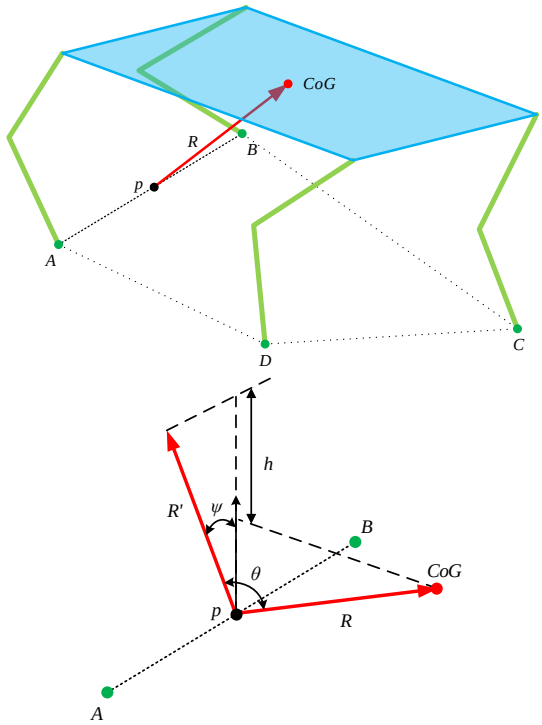

Figure 4. A diagram illustrating the support boundary ABCD of a quadruped robot (top) and a visualization of the normalized energy stability margin *h* for the line segment AB (bottom).

formed by two footholds A and B, let the midpoint of the line segment be p, and the vector from p to the robot's center of gravity be R. Vector R may be rotated about the line AB by θ such that R lies in the plane formed by AB and the unit vector $\hat{z}$ that defines the upward direction in the space. R', the rotated vector R now lying in this plane, can be rotated about R by ψ to align with $\hat{z}$. Then, the normalized energy stability margin is h, the effective height the robot's center of gravity must overcome by rotating or toppling about line AB.

$$S_{NE} = |R|(1 - \cos\theta)\cos\psi \qquad (9)$$

Geometrically speaking, the energy stability margin decreases as the center of gravity moves horizontally closer to the plane. Therefore, it is important to minimize the difference between the energy stability margin of the line segments during locomotion as in [9]. This task becomes even more critical for robots with underactuated legs since the reconfiguration along the energy gradient can further decrease the energy stability margin for certain line segments. Consequently, this imposes constraints on the parameters of the alternating stance gait since each horizontal movement of the center of gravity must not result in falling below a certain energy stability margin for the current support boundary or the next support boundary. In this work, the gait parameters that affect the movement of the center of gravity such as the horizontal stroke with each translation and the prismatic leg actuation were manually prescribed for the

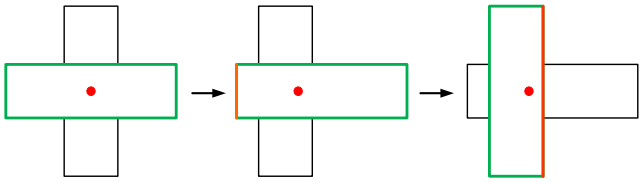

Figure 5. Energy stability margin of the stance platform edges throughout the gait cycle. As the swing phase platform (black) translates, the center of mass (red) moves closer to the front edge (orange), decreasing its stability margin. Upon switching the stance platform, the rear edge (dark orange) has an even lower stability margin.

experiment; however, we note that determining the optimal gait parameters would require online estimation of friction and a priori knowledge of the terrain.

MECHANICAL DESIGN OF THE ROBOT

The robot consists of two quadruped platforms that translate and rotate relative to each other for locomotion as shown in Figure 6. They are joined perpendicularly to achieve a compact form factor and to prevent interference during locomotion. The robot has a total of four Dynamixel motors: one to actuate the four legs on each of the two platforms and two to actuate the translational and rotational motions. The steering is not demonstrated in this work since it does not relate to passive adaptability to terrain.

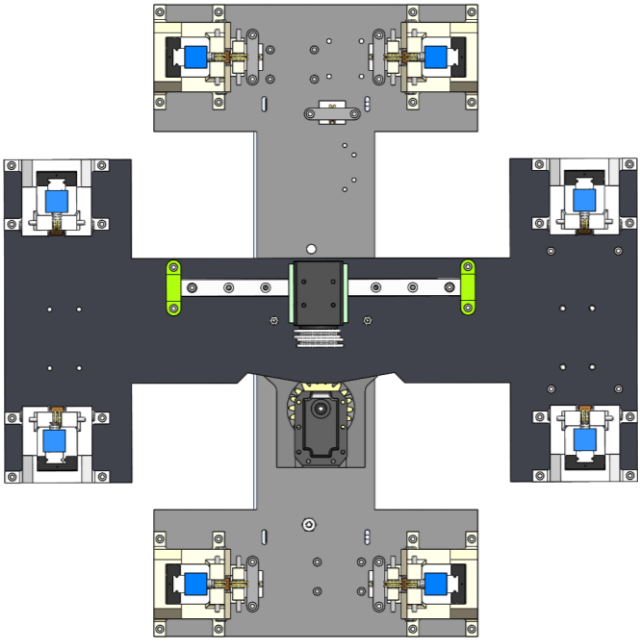

Figure 6. A top view of the robot showing the two quadruped platforms placed one on top of another. The perpendicular orientation minimizes interference during locomotion while allowing a compact assembly.

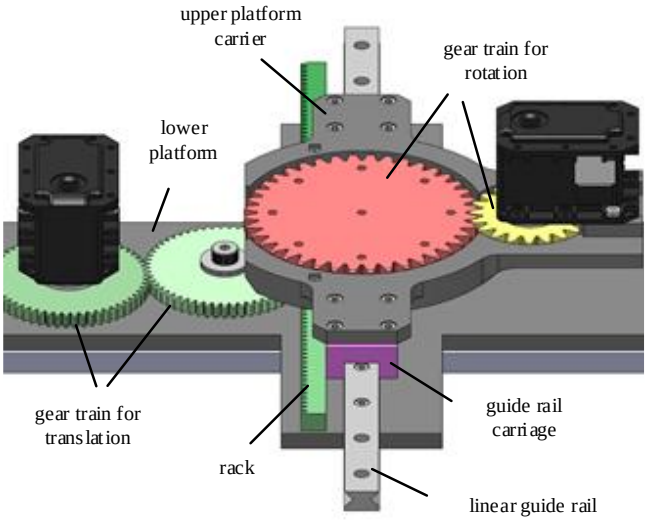

Figure 7. The locomotion mechanism that lies between the two platforms. The left motor actuates the translation via the gear train and rack (green), and the right motor actuates the rotation via the gear train (red and yellow) embedded in the upper platform carrier. The upper platform (hidden to reveal the mechanism) sits on the red gear.

The locomotion mechanism for the robot is designed to minimize the difference in height between the two platforms, the center of mass height, and the overall size. Therefore, it is placed between the upper and lower platforms and consists of custom gears to minimize the mechanism's vertical dimension. The upper platform sits on a spur gear embedded in a carrier that can slide on a linear guide rail. The spur gear in the carrier facilitates the rotation while the linear guide rail facilitates the translation. A view of the locomotion mechanism is shown in Figure 7.

The prismatic legs are implemented using a ball bearing linear guide rail. The prismatic leg has two anchor points: one at the top for the actuation cable and another at the bottom for the constant force spring. A rounded rubber pad is attached at the foot for traction. The guide rail carriage, pulley and the constant force spring for the leg are installed in a 3D printed part. The

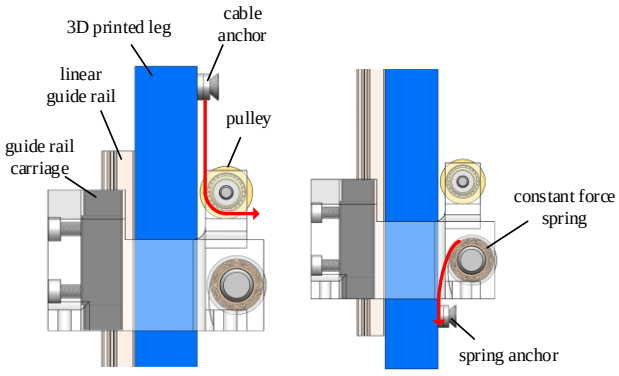

Figure 8. Side views of the prismatic leg in the mount assembly. The actuation cable (red/left) anchored at the top moves downward, and the constant force spring anchored at the bottom extends downward (red/right).

motion of the prismatic leg, actuation cable and the constant force spring is shown in Figure 8.

Tension in the cables is kept constant throughout actuation by routing them only at right angles around the pulleys. The adaptive coupling between the two pulley differentials is formed on the upper platform by allowing the motor to move on a linear rail. The lower platform, however, does not have the space for the same design since that would cause the underside of the robot to collide with the terrain. Instead, the lower platform uses an additional pulley differential to couple the two floating pulley differentials. As a result, the cable routing for the lower platform lies underneath the body.

The motors are controlled by a U2D2 unit produced by Robotis for the Dynamixel motors. A Raspberry Pi 3 B+ interfaces this unit via USB, and the robot is remotely controlled via an SSH connection. The electrical components receive power through the cords running up to the robot. Because the cords are lightweight, they do not affect the motion of the robot.

EXPERIMENTS

To measure the robot's ability to passively adapt to terrain, two types of experiment were conducted. In the first experiment, the robot maneuvered two different unstructured terrains: (1) a mound-like pile of wooden blocks similar to that shown in Figure 1 and (2) a set of wooden blocks of different heights randomly scattered across a flat surface as shown in Figure 9. The wooden blocks are approximately 1.5" × 4" × 0.5" in size, and the tallest obstacle in the two terrains measured approximately 2.5". In the second experiment, the robot stood on four stance legs while wooden blocks of increasing height were placed under two swing legs: opposing legs and diagonal legs. The swing legs were then actuated to observe the changes in the body posture and quantify the passive adaptability of the prismatic legs to different terrain elevations.

To measure the robot's body posture over time, an MPU-9250 9-axis inertial measurement unit was mounted on the upper platform. The Raspberry Pi sampled the accelerometer, gyroscope, and magnetometer of the IMU at 500 Hz, and a

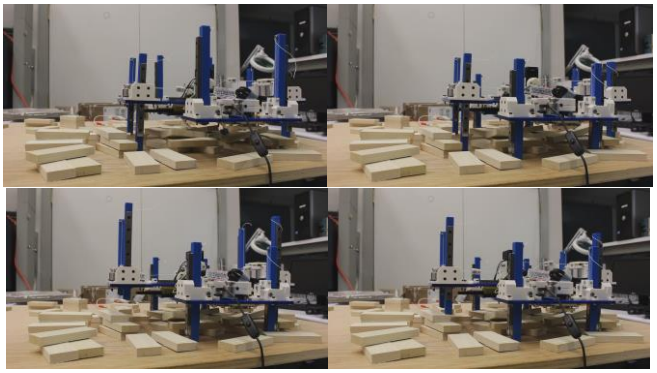

Figure 9. Images of the underactuated legged robot maneuvering an unstructured obstacle course. The robot begins with one platform in stance phase (upper left) and switches the two platforms (upper right). The swing phase platform translates (lower left), and switching occurs again (lower right).

gradient descent algorithm for the estimation of IMU orientation proposed by Madgwick et al. [11] was used to determine the ZYX Euler angles of the robot based on the IMU measurements. For the experiments on maneuvering unstructured terrains, calibration weights were placed on the robot to compensate for the uneven mass distribution of the robot design.

RESULTS

Figures 10 and 11 show the changes in the pitch and roll angles of the body as the robot maneuvered the two terrains in the first experiment. The data collected on the Raspberry Pi was imported into MATLAB for processing by removing the outliers and smoothing the data. Because the terrains were arbitrarily made without any consideration of the sequential placement of the feet, the robot encountered several challenging situations throughout locomotion such as a ground contact made only at the corner of a foot and the terrain collapsing under the feet due to wooden blocks slipping and falling down from their placed locations. Despite these unfavorable conditions, the prismatic legs maintained the stability of the robot by mostly exerting forces perpendicular to the contact location.

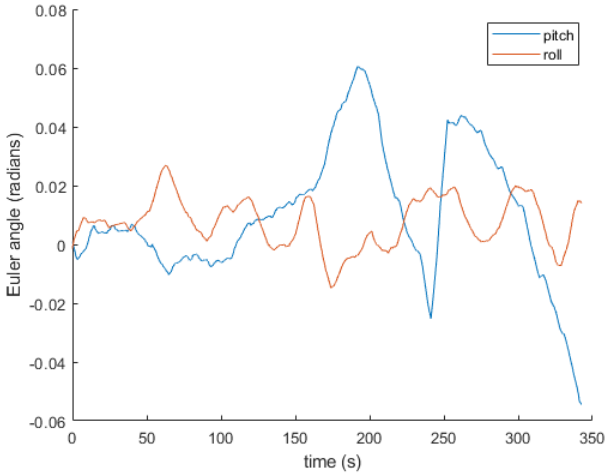

Figure 10. Pitch and roll of the robot over an unstructured, mound-like terrain.

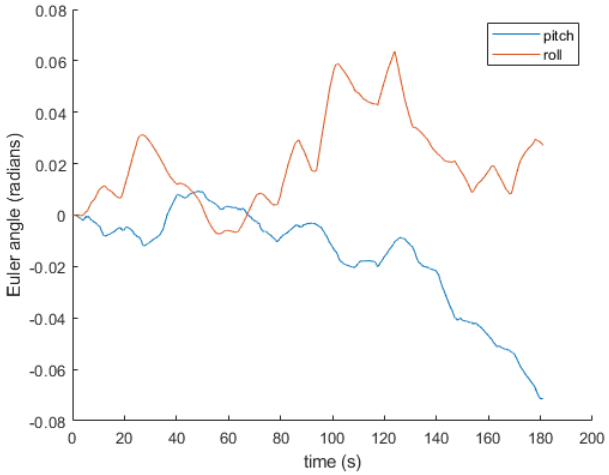

Figure 11. Pitch and roll of the robot over an unstructured terrain with scattered obstacles.

Figure 10 shows that the robot maintained a fairly steady roll angle whereas the pitch angle adjusted to the overall slope of the current terrain. As the robot moved up the incline of the first terrain, the pitch angle gradually increased. After walking over the highest point of the terrain, the robot began to slightly pitch down. When the rear legs of the robot suddenly fell down due to the terrain collapsing around 250 s, the pitch angle suddenly increased before the robot resumed pitching down.

In Figure 11, the roll angle changed according to the differences in the terrain elevation between the left and right sides, but the pitch angle gradually became more negative. It was observed during this experimental trial that the deflection of the upper platform during its stance phase caused its prismatic legs to slightly point outward. Because the terrain in the experimental trials consisted of scattered obstacles freely placed on a surface, the small outward rotation of the prismatic legs pushed the wooden blocks away, resulting in the feet slipping on the terrain and pitching down every time.

TABLE 1: CHANGE IN PITCH AFTER GROUND CONTACT FOR DIFFERENT TERRAIN ELEVATIONS

Terrain height	Opposing legs	Diagonal Legs
0.5”	0.0016	0.0086
1.0”	0.0078	0.0053
1.5”	0.0067	0.0046
2.0”	0.0038	0.0051

TABLE 2: CHANGE IN ROLL AFTER GROUND CONTACT FOR DIFFERENT TERRAIN ELEVATIONS

Terrain height	Opposing legs	Diagonal Legs
0.5”	0.0010	0.0003
1.0”	0.0010	-0.0007
1.5”	-0.0009	-0.0001
2.0”	0.0030	-0.000071

Table 1 and 2 show the change in the robot body’s pitch and roll angles after the swing legs contacted the ground. The first and second columns contain the values for the trials in which the wooden blocks were placed under two adjacent, opposing legs and under two diagonal legs respectively. The data indicates that the underactuated legged robot can passively adapt to the terrain particularly well when stationary. The data also suggest that the higher changes in the pitch and roll angles shown in Figures 10 and 11 may be due to the gradual tipping of the body caused by the feet slipping on the terrain during locomotion.

CONCLUSION AND FUTURE WORK

In this paper, we presented the design of an underactuated legged robot with prismatic legs that can maneuver unstructured terrains in open-loop control. The novel leg design motivated by previous underactuated leg designs and an analysis of the energy model was shown. An actuation scheme that leverages the passive adaptability in the leg mechanism allowed the robot to maintain its body posture as it traversed unstructured obstacle

courses, as demonstrated in the experimental results. The robot experienced maximum deviations of 4.94º and 4.17º from its original pitch and roll angles respectively while maneuvering the two unstructured terrains. The robot demonstrated a greater ability to passively adapt to terrains when stationary with maximum deviations of 0.45º and 0.49º in the pitch and roll angles respectively.

The current robot design has several limitations that restricts its locomotion speed. Because the moving center of mass during translation can significantly decrease the energy stability margin, the robot's stride per gait cycle is greatly limited. Moreover, the period of the gait cycle is nearly doubled due to the intermediate actuation phase, which was necessary to minimize the net moment on the robot body during switching. The robot would clearly benefit from a passive mechanism that can resist reconfiguration in the legs during locomotion. Another limitation is that the robot does not have a passive leveling ability. Therefore, changes in the body posture accumulate over time and can eventually result in toppling.

In future works, we will incorporate a passive mechanism that can maintain the passive adaptability of the prismatic legs without sacrificing the locomotion speed. The mechanism should also increase the robot's robustness to any external disturbance such that the accumulation of posture changes over time is minimal.

ACKNOWLEDGMENTS

This work was funded in part by the National Science Foundation, grant IIS- 1637647.

The authors would like to thank Neil Bajaj and Walter Bircher for their mentorship during this project.

REFERENCES

[1] G. Bledt, P. M. Wensing and S. Kim, "Policy-regularized model predictive control to stabilize diverse quadrupedal gaits for the MIT cheetah," 2017 IEEE/RSJ International Conference on Intelligent Robots and Systems (IROS), Vancouver, BC, 2017, pp. 4102-4109.

[2] Saranli, U., Buehler, M., and Koditschek, D. E., 2001, "RHex: A Simple and Highly Mobile Hexapod Robot," Int. J. Rob. Res., 20(7), pp. 616–631.

[3] Cham, J. G., Bailey, S. A., Clark, J. E., Full, R. J., and Cutkosky, M. R., 2002, "Fast and Robust: Hexapedal Robots via Shape Deposition Manufacturing," Int. J. Rob. Res., 21(10-11), pp. 869–882.

[4] B. G. Buss, A. Ramezani, K. Akbari Hamed, B. A. Griffin, K. S. Galloway and J. W. Grizzle, "Preliminary walking experiments with underactuated 3D bipedal robot MARLO," 2014 IEEE/RSJ International Conference on Intelligent Robots and Systems, Chicago, IL, 2014, pp. 2529-2536.

[5] C. S. Casarez and R. S. Fearing, "Steering of an Underactuated Legged Robot through Terrain Contact with an Active Tail," 2018 IEEE/RSJ International Conference on Intelligent Robots and Systems (IROS), Madrid, 2018, pp. 2739-2746.

[6] Y. Kanner, Oren & M. Dollar, Aaron. (2012). Optimization of Coupling Ratio and Kinematics of an Underactuated Robot Leg for Passive Terrain Adaptability. 4. 10.1115/DETC2012-70741.

[7] Y. Kanner, Oren & Odhner, Lael & M. Dollar, Aaron. (2014). The design of exactly constrained walking robots. Proceedings - IEEE International Conference on Robotics and Automation. 2983-2989. 10.1109/ICRA.2014.6907289.

[8] McGhee, R. B. and Frank, A. A. On the stability properties of quadruped creeping gaits, Mathematical Bioscience, Vol. 3, pp. 331-351, 1968.

[9] A. Messuri, Dominic & A. Klein, Charles. (1985). Automatic body regulation for maintaining stability of a legged vehicle during rough-terrain locomotion. Robotics and Automation, IEEE Journal of. 1. 132 - 141. 10.1109/JRA.1985.1087012.

[10] Hirose, Shigeo & Tsukagoshi, Hideyuki & Yoneda, Kan. (2001). Normalized energy stability margin and its contour of walking vehicles on rough terrain. Proceedings - IEEE International Conference on Robotics and Automation. 1. 181 - 186 vol.1. 10.1109/ROBOT.2001.932550.

[11] S. O. H. Madgwick, A. J. L. Harrison and R. Vaidyanathan, "Estimation of IMU and MARG orientation using a gradient descent algorithm," 2011 IEEE International Conference on Rehabilitation Robotics, Zurich, 2011, pp. 1-7.